Nanochem Res 6(2): 188-201, Summer and Autumn 2021

RESEARCH PAPER

Efficient reduction of hexavalent chromium and 4-nitrophenol using Ag NPs/Zeolite 13X nanocomposite as a green and retrievable catalyst

Bahar Khodadadi [1*], Maryam Bordbar[1], Ali Yeganeh Faal[2], Fatemeh Rahmi[2], Bahareh Derakhshan[1]

[1] *Department of Chemistry, Faculty of Science, University of Qom, Qom, Iran*

[2] *Department of Chemistry, Faculty of Science, Payame Noor University, Qom, Iran*

ARTICLE INFO

Article History:
Received 02 July 2021
Accepted 27 September 2021
Published 15 October 2021

Keywords:
Ag nanoparticles
Zeolite 13X
NaBH4
4-NP
Cr (VI)

ABSTRACT

In the present study, the Ag NPs/Zeolite 13X nanocomposite as an effective catalyst was prepared through the reduction of Ag+ ions using Tragopogon graminifolius extract as the reducing and stabilizing agent and Ag NPs immobilization on Zeolite 13X surface in the absence of any stabilizer or surfactant. Several techniques such as FT-IR spectroscopy, UV-Vis spectroscopy, X-ray Diffraction (XRD), Scanning Electron Microscopy (FE-SEM), Energy Dispersive X-ray Spectroscopy (EDS), and Transmission Electron Microscopy (TEM) were used to characterize Zeolite 13X, Ag NPs, and Ag NPs/ Zeolite 13X. Moreover, the catalytic activity of the Ag NPs/Zeolite 13X nanocomposite was investigated in the reduction of 4-nitrophenol (4-NP) and chromium (VI) at room temperature. According to the experimental results in this study, Ag NPs/Zeolite 13X nanocomposite was found to be of high catalytic activity. In addition, Ag NPs/Zeolite 13X nanocomposite can be recovered and reused several times in the reduction of 4-NP and chromium (VI) with no significant loss of catalytic activity.

How to cite this article
Khodadadi B., Bordbar M., Yeganeh Faal A., Rahmi F., Derakhshan B. Efficient reduction of hexavalent chromium and 4-nitrophenol using Ag NPs/Zeolite 13X nanocomposite as a green and retrievable catalyst. Nanochem Res, 2021; 6(2):188-201. DOI: 10.22036/ncr.2021.02.006

INTRODUCTION

Water pollution, caused by the improper discharge of urban and industrial waste, toxic pollutants and improper management of solid waste, can have serious impacts on human health. Nitrophenol compounds are refractory pollutants in wastewater that are widely used in a variety of industries including ceramics, cosmetics, textiles, paper, and enterprises that manufacture explosives. Nitrophenol compounds, such as 4NP, have been demonstrated to be capable of damaging the central nervous system, liver, kidneys, and blood in humans and animals. Hexavalent chromium (Cr (VI)) is one of the toxic heavy metals with carcinogenic and mutagenic activity generated in industrial processes such as tanned metal electroplating and pigment manufacturing [1-4]

Traditional wastewater treatment methods, such as adsorption and chemical coagulation, which are two common techniques for wastewater treatment, only transfer pollutants from the liquid to the solid phase. This can cause secondary contamination and requires additional treatment [5].

One of the most effective methods for removing toxic, bio-refractory, chemically stable and carcinogenic pollutants such as 4-NP in wastewater is the reduction of these compounds in the presence of metal nanoparticles (MNPs) and $NaBH_4$. Thus, an effective method for 4-NP reduction using

* Corresponding Author Email: *: Bkhodadadi98@yahoo.com*

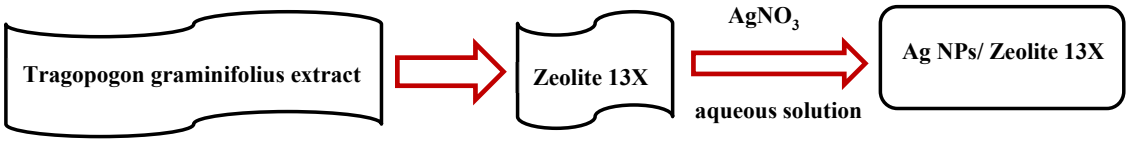

Scheme 1. Diagrammatic synthesis of the Ag NPs/Zeolite 13X nanocomposite using Tragopogon graminifolius extract

metal nanoparticles have recently received a lot of attention due to its cost-effectiveness [4-9].

It is well-known that silver NPs exhibit unique physical, chemical, thermodynamic and optical properties, which make them useful in many fields such as catalysis, gas sensors, batteries, solar energy conversion tools, high-temperature superconductors, biosensing, antibacterial, antiviral and antifungal activities, drug delivery, etc. [10-15]. In addition, silver nanoparticles have a high surface-to-volume ratio that can dramatically increase the interaction between reactants and catalysts. Heterogeneous catalysts are also increasingly used in the form of the M NPs due to their higher existing catalyst surface area. Additionally, heterogeneous nanocatalysts can easily separate products from the reaction mixture to form recyclable catalysts [16-18]. However, the agglomeration of the M NPs is a major problem, which can be overcome using ideal supports. In order to prevent the agglomeration of the M NPs and overcome the problems related to their stability, separation, and recovery, several inorganic compounds including graphene oxide, various types of zeolites, TiO_2 and Fe_3O_4 have been applied as M NPs supports [19-23]. However, to date, there has been no report about Zeolite 13X as support. Thus, the present study is reporting the Zeolite 13X due to its good chemical and thermal stability, low cost, low toxicity and excellent optical properties.

Several physical and chemical techniques are applied for the synthesis of the M NPs. However, these methods have some disadvantages such as long reaction times, high temperature, use of expensive, hazardous and toxic agents or stabilizers, environmental pollution caused by the utilization of organic solvents, and low product yields [24-29].

Recently green synthesis of the MNPs has received much attention owing to several advantages such as simple methodology, cost-effectiveness, environmental friendliness, very moderate reaction conditions, being organic solvent-free, easy to work up and suitably scaled up [16]. It is worth noting that, plant extracts act both as reducing and capping agents in the synthesis of nanoparticles [15, 16, 30-36]. Several plants have been successfully used for the rapid and efficient synthesis of NPs from extracellular Ag [16, 19, 35]. To date, the biosynthesis of NPs from Ag using the Tragopogon graminifolius extract has not been reported.

The family Trragopogon graminifolius DC. Compositae is well known in traditional Iranian medicine (TIM) as "Sheng" or "Lachiatotis". Its aerial parts, including leaves and stems, are widely used as greens and various local products in western Iran. It has been used to treat wounds, bleeding, and various digestive and liver disorders in TIM. The hydroalcoholic extract of the roots and aerial parts of the plant exhibits powerful antioxidant activity and is rich in polyphenolic compounds. It can also be used as an important source for the biosorption of metal ions and the production of nanoparticles [37-39].

In this study an environmentally friendly, non-toxic and clean method is used for the first time for the green synthesis of the Ag NPs/Zeolite 13X nanocomposite using Tragopogon graminifolius in the absence of any stabilizer or surfactant (Scheme 1). The Ag NPs/Zeolite 13X nanocomposite was utilized for the reduction of 4-NP and Cr (VI) in water at room temperature.

EXPERIMENTAL METHOD

Instruments and reagents

All chemical reagents were purchased from the Merck and Aldrich Chemical Companies. All materials were of commercial reagent grade. A Nicolet 370 FT/IR spectrometer (Thermo Nicolet, USA) using pressed KBr pellets recorded FT-IR spectra. To record UV-visible spectra in the wavelength range of 200-700 nm, a Shimadzu UV-2500 double-beam spectrophotometer was used. X-ray diffraction (XRD) measurements were carried out using a Philips model X'Pert Pro diffractometer type PW 1373 goniometer (Cu Kα = 1.5406 A˚). The scanning rate was 2º/min in the 2θ range from 10 to 90˚. Particle dispersion morphology were investigated by scanning electron microscopy (SEM) (Cam scan MV2300). EDS (Energy

Fig. 1. Image of Tragopogon graminifolius

Dispersive X-ray Spectroscopy) performed in SEM were used for measuring the chemical composition of the prepared nanostructures. Transmission electron microscope (TEM) using a Philips EM208 microscope operating at an accelerating voltage of 90 kV were used for identifying the size and shape of the prepared Ag NPs.

Preparation of Tragopogon graminifolius extract

15 g of dried, powdered Tragopogon graminifolius were added to 100 mL of 75% (V/V) ethanol solution at 70°C over a period of 30 min. After that, the mixture was allowed to cool to room temperature. Then, the extract of Tragopogon graminifolius was centrifuged at 6500 rpm and the supernatant was separated by filtration.

Preparation of the Ag NPs using Tragopogon graminifolius extract

For green synthesis of the Ag NPs, 0.02 g $AgNO_3$ was dissolved in aqueous media. Then, the prepared aqueous solution of $AgNO_3$ was added dropwise to 50 mL of Tragopogon graminifolius extract under constant stirring at 80 °C by changing the color of the mixture. The reduction of silver ions (Ag^+) to silver (Ag^o) completed in about 30 min, as monitored by UV-Vis and FT-IR spectra of the reaction mixture**.** The color of the reaction mixture gradually changed in 15 min at 80 °C, indicating the formation of silver nanoparticles. Finally, the colored solution of silver nanoparticles was then centrifuged at 6500 rpm for 30 min for complete separation.

Preparation of the Ag NPs/ Zeolite 13X

0.5 g of Zeolite 13X powder was dispersed in 50 mL of Tragopogon graminifolius extract under constant stirring at ambient temperature for 15 min. Afterward, 20 mL of a 0.03 M aqueous solution of $AgNO_3$ was added dropwise to the prepared mixture and the reaction mixture was heated under traditional reflux conditions for 2 h at 80 °C. The reaction mixture was allowed to cool; the formed precipitate was filtered and collected over a round dish. Finally, it was washed several times with distilled water and once with ethanol and air, dried at 50 °C for 24 h in an oven, and then characterized.

Reduction of 4-NP

A typical 25 mL of 2.5 mM aqueous solution of the 4-NP and 3.0 mg of the Ag NPs/Zeolite 13X nanocomposite were mixed at room temperature under constant stirring for 2 min. Then, 25 mL of the freshly prepared NaBH4 solution (0.25 M) was added to the contents of the baker and the reaction process was monitored using UV-Vis spectrophotometer and through recording λmax changes at 400 nm. When the color of the solution disappeared, the catalyst was separated from the reaction mixture, washed, dried and then reused for the next run.

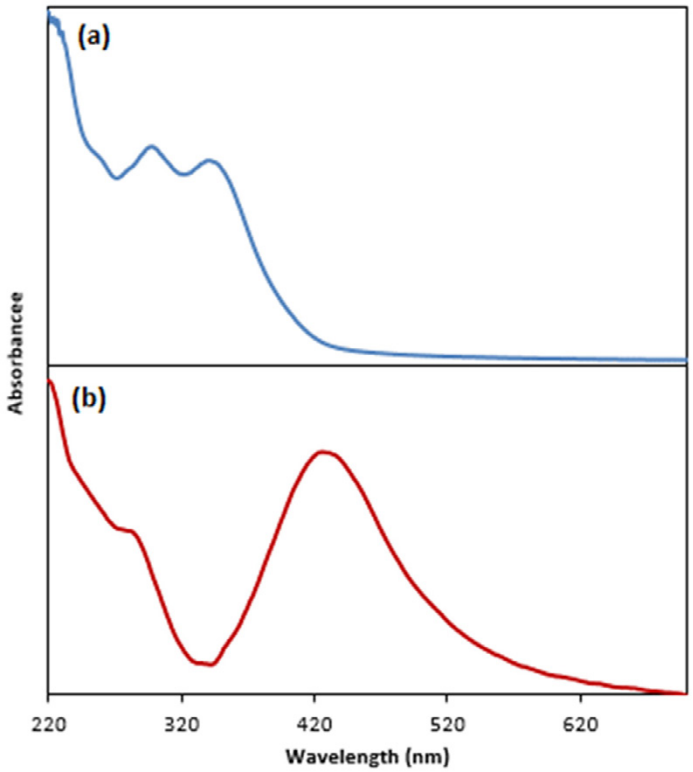

Fig. 2. UV-Vis spectrum of Tragopogon graminifolius extract (a), and green synthesized Ag NPs using Tragopogon graminifolius extract (b)

Reduction of Cr (VI)

Typically, various amounts of Ag NPs/Zeolite 13X nanocomposite and 25 mL of 3.4 mM aqueous solution of Cr (VI) were added to 1.0 mL formic acid solution (88%) at room temperature under constant stirring. The Cr (VI) concentration was then determined using an indirect UV–visible spectrophotometric method based on the reaction of Cr (VI) and diphenylcarbazide, which forms a red–violet colored complex. Finally, the absorbance of the colored complex was measured in a double beam spectrophotometer at 540 nm wavelength [40].

RESULTS AND DISCUSSION

Tragopogon graminifolius extract and green synthesized Ag NPs were characterized by UV-Vis and FT-IR analysis. Fig. 2 (a) shows the UV two bonds of the extract at 292 nm and 335 nm due to the cinnamoyl and benzoyl systems, respectively. In fact, they are concerned with the $\pi \rightarrow \pi^*$ transitions of polyphenolics [15, 16]. The surface plasmon resonance (SPR) signal at about 430 nm, in the UV-Vis spectrum of biosynthesized Ag NPs after changing the color of the solution demonstrates the formation of Ag NPs (Fig. 2(b)) [41-43].

The FT-IR of the Tragopogon graminifolius extract (Fig.3 (a)) shows signals around 3450, 1725, 1596 and 1386 to 1066 cm^{-1} indicating the OH, carbonyl group (C=O), C=C aromatic ring and C-OH, C-C and C-H vibrations, respectively [4, 41]. Owing to the presence of these functional groups in the structure of polyphenolics, which exist in Tragopogon graminifolius extract, it can be concluded that the phenolics in the extract are probably responsible for the reduction of Ag^+ and formation of the corresponding Ag. According to the results obtained from the FT-IR study of green synthesized Ag NPs using Tragopogon graminifolius extract (Fig. 3(b)), the positions of observed peaks are almost similar to those of the corresponding peak in the FT-IR spectrum of Tragopogon graminifolius extract. These signals clearly confirm the presence of plant phytochemicals on the surface of Ag NPs and their effects on the protection and stability of NPs.

As Fig.4 shows, the strong peak observed at around 1066 cm^{-1} in the spectra of the Zeolite

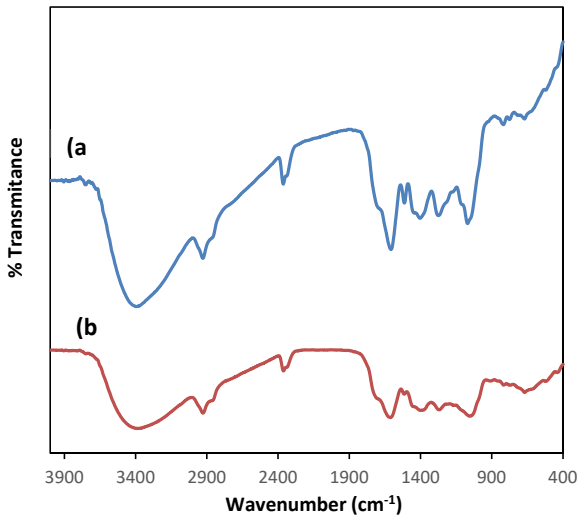

Fig. 3. FT-IR spectrum of Tragopogon graminifolius extract (a), and green Ag synthesized NPs using Tragopogon graminifolius extract (b).

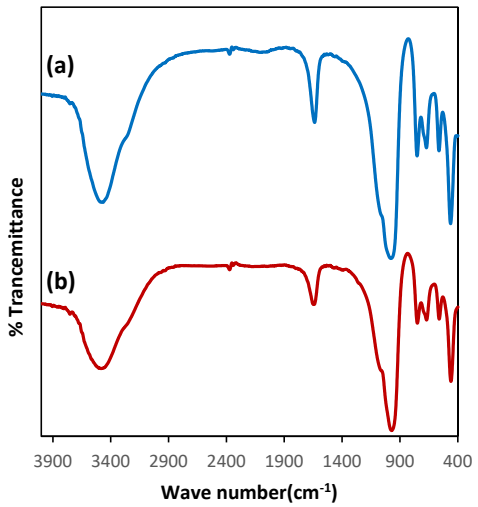

Fig. 4. FT-IR spectrum of (a) the Zeolite 13X; (b) Ag NPs/Zeolite 13X nanocomposite samples.

13X and Ag NPs/Zeolite 13X nanocomposite corresponds to the stretching vibration of -Si-O-Si- bond overlaps with the stretching vibration of -Al-O- and -Al-O-Si- bonds. The stretching modes, located in the region of 620-740 cm^{-1} which can be associated with the tetrahedral atoms, are sensitive to the Si-Al composition of the framework and may shift to lower frequencies as the number of tetrahedral aluminum atoms increases. The bands related to pseudo-lattice vibrations of structural units are observed in the range of 500-700 cm^{-1} [35, 44] in the FT-IR spectra of the zeolitic structure.

The FT-IR analysis of Ag NPs/Zeolite 13X nanocomposite (Fig. 4 (b)) shows that no changes occur in the functional groups following the Ag NP immobilization on Zeolite 13X compared with Zeolite 13X. The antioxidant action of flavonoids resides mainly in their ability to donate electrons or hydrogen atoms (Scheme 2). In this work, the Ag(I) ions were reduced to Ag(0) metallic particles by flavonoids and phenolics present in Tragopogon graminifolius extract according to the following mechanism. Flavonoids and other phenolics present in the extract are not only facilitating the formation of pure Ag NPs by the reduction of the Ag(I) to Ag(0) but also provide excellent tenacity

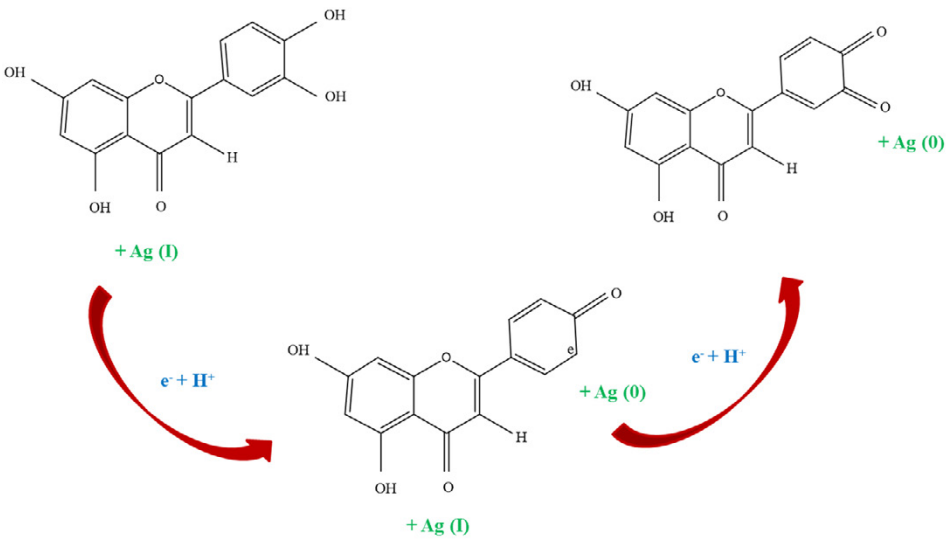

Scheme 2. Mechanism for green synthesis of Ag NPs using Tragopogon graminifolius extract

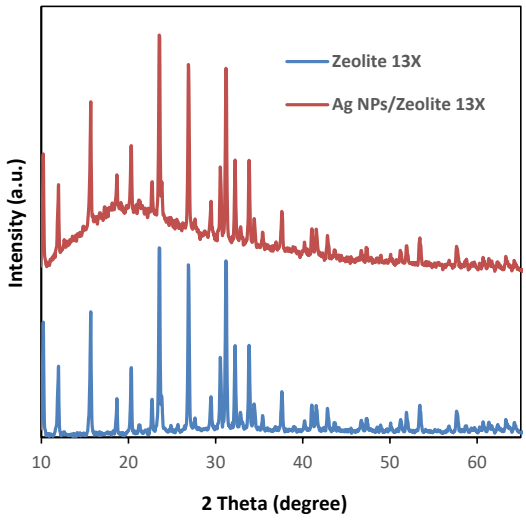

Fig. 5. XRD pattern of the Zeolite 13X and Ag NPs/Zeolite 13X nanocomposite samples

against agglomeration.

Moreover, Fig. 5 represents the XRD pattern of the Ag NPs/ Zeolite 13X. On the basis of the above results, the diffraction peaks at 38.73°, 44.26°, 64.59°, and 78.12° are consistent with the metallic silver particles and well-matched with JCPDS card of Ag (NO. 04-0783), which exhibits face-centered cubic (FCC) structure of the metallic silver NPs immobilized on the surface of Zeolite 13X without the formation of impurities such as silver oxide (Ag_2O) [4, 42].

Scanning electron microscopy (SEM) analysis was employed in order to determine the size and morphologies of both Zeolite 13X and Ag NPs/ Zeolite 13X. Fig. 6 shows a typical FE-SEM image of the samples. These images indicate that the Ag NPs and Zeolite 13X manifest spherical morphology with diameters of less than 20 nm with very narrow diameter distributions. From SEM images, it is clear that Ag NPs are deposited on the surface of Zeolite 13X without being incorporated in Zeolite 13X.

The elemental composition of the Ag NPs/ Zeolite 13X nanocomposite was also characterized

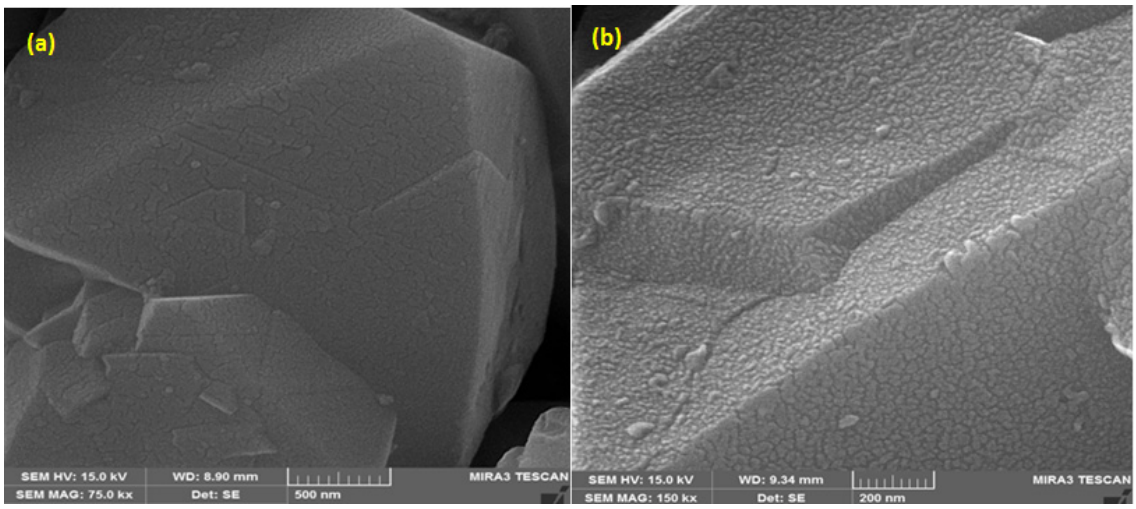

Fig. 6. FE-SEM image of (a) Zeolite 13Xand (b) Ag NPs/Zeolite 13X nanocomposites

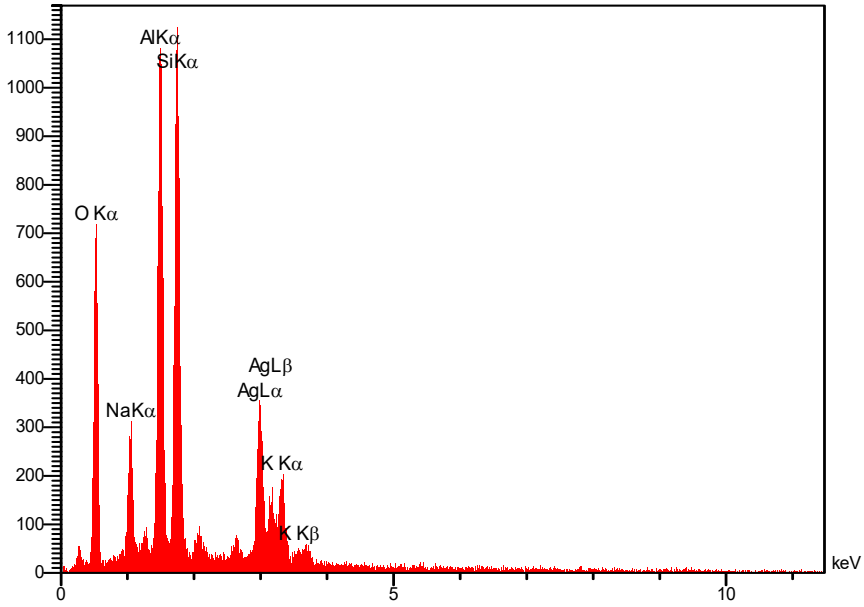

Fig. 7. EDS spectrum of the Ag NPs/Zeolite 13X nanocomposite.

by EDS spectrum (Fig. 7). Fig. 7 confirms the presence of Na, Al, O, Si and Ag elements in the Ag NPs/ Zeolite 13X. Moreover, Fig. 8 illustrates the elemental mapping images, which demonstrate that Ag NPs are dispersed on the surface of the Ag NPs/ Zeolite 13X.

Transmission electron microscopy (TEM) was carried out in order to perform a more detailed study of the morphology and size of the Ag NPs/ Zeolite 13X nanocomposite sample. Fig. 9 shows the TEM image of typical Ag NPs/ Zeolite 13X, in which Ag nanoparticles appear as dark dots over the surface of Zeolite 13X with average sizes of less than 20 nm.

According to the obtained results, we propose a structure for the nanocomposite in which the Ag NPs have been embedded in the glass matrix (Scheme 3). Zeolite 13X has some regular holes as well, and an appropriate interaction can be occurred between the empty orbital of Si with P-orbital electron pairs of the metal or among electron pairs of oxygen with P-empty orbital of the metal.

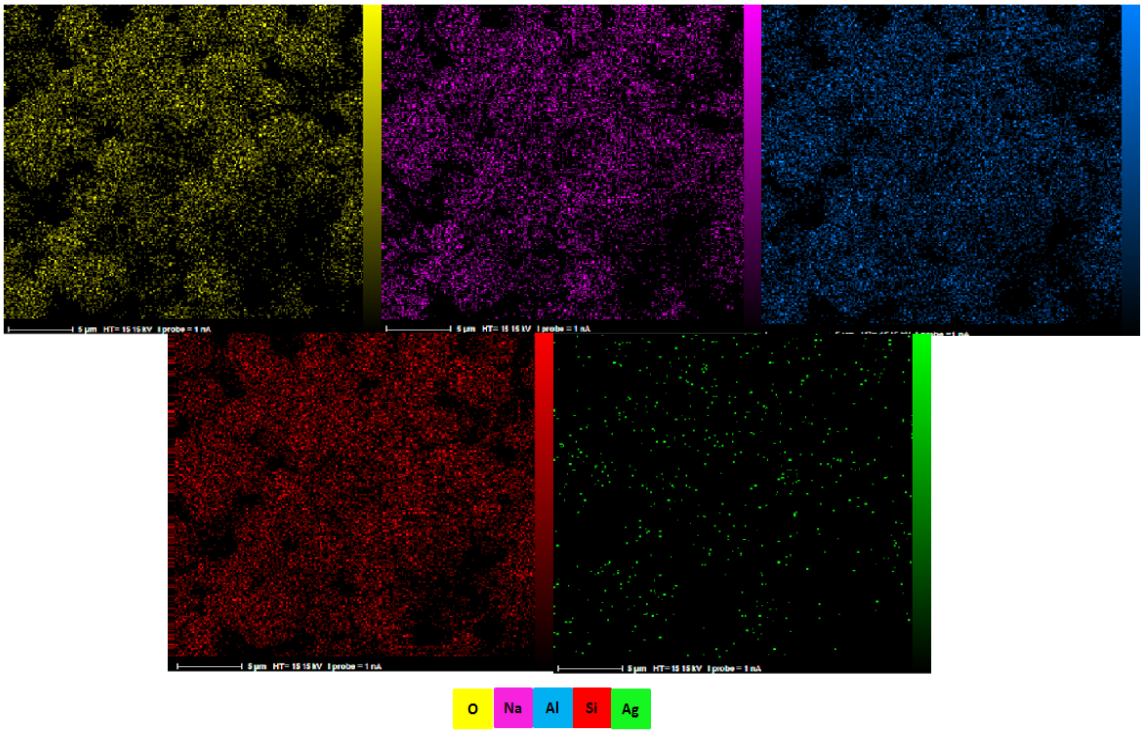

Fig. 8. Elemental mapping of the Ag NPs/Zeolite 13X nanocomposite.

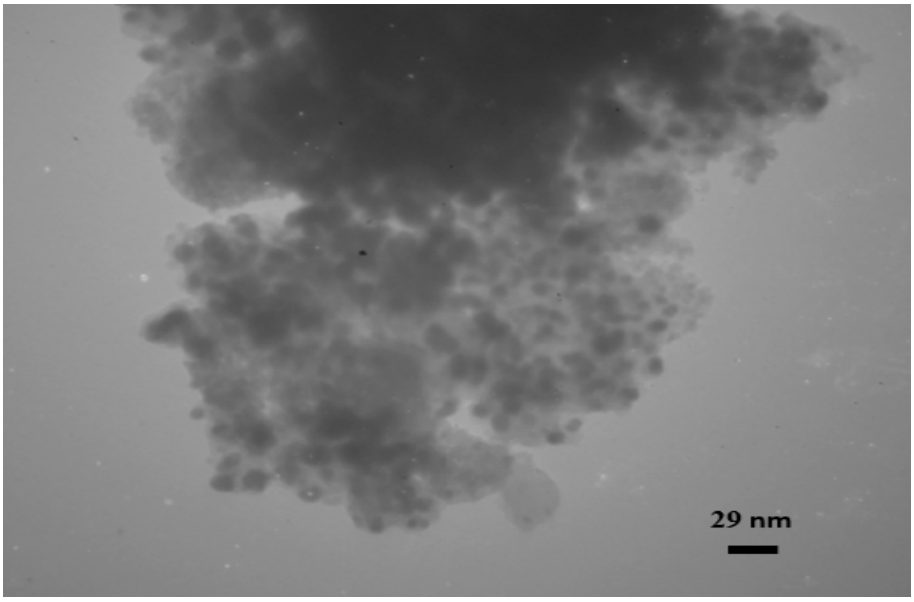

Fig. 9. TEM image of the Ag NPs/Zeolite 13X nanocomposite

Evaluation of catalytic activity of the Ag NPs/ Zeolite 13X nanocomposite through the reduction of 4-NP

In this study, the catalytic performance of the Ag NPs/Zeolite 13X nanocomposite was evaluated through the reduction of 4-NP in the presence of excess amounts of $NaBH_4$. According to UV-Vis spectrum, the aqueous solution of 4-NP exhibits an intense absorption about at 315 nm in neutral or acidic media. After the addition of $NaBH_4$, a red shift of the peak of 4-NP from 315 to 400

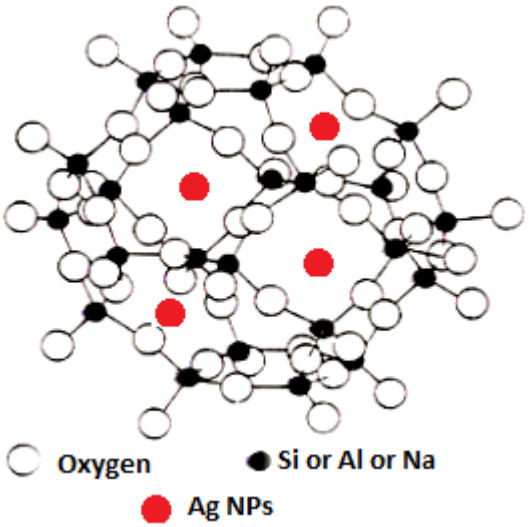

Scheme 3. Proposed structure of the Ag NPs/Zeolite 13X nanocomposite

Table 1. Completion time for the reduction of 4-NP (2.5 mM) to 4-AP.

	Catalyst	[$NaBH_4$](mM)	Time (min)
1	-	250	150*
2	Zeolite 13X (10 mg)	250	150*
3	Ag NPs (10 mg)	250	21
4	Ag NPs/Zeolite 13 X (5 mg)	125	10:23
5	Ag NPs/Zeolite 13 X (5 mg)	187.5	5:41
6	Ag NPs/Zeolite 13 X (5 mg)	250	4:52
7	Ag NPs/Zeolite 13 X (7 mg)	125	6:19
8	Ag NPs/Zeolite 13 X (7 mg)	187.5	3:21
9	Ag NPs/Zeolite 13 X (7 mg)	250	2:40
10	Ag NPs/Zeolite 13 X (10 mg)	125	3:19
11	Ag NPs/Zeolite 13 X (10 mg)	187.5	2:53
12	Ag NPs/Zeolite 13 X (10 mg)	250	1:37

*: Not completed

nm was observed and the color of the solution altered from light yellow to deep yellow due to the formation of 4-nitrophenolate ions under strong basic conditions. The effects of $NaBH_4$ and catalyst concentrations and various amounts of catalyst and $NaBH_4$ on the catalytic reduction of 4-NP to 4-AP were studied, and the results are shown in Table 1. In the absence of the catalyst, the λ_{max} of 4-nitrophenolate remains unchanged even after 150 min. To study the effect of support and Ag NPs on the efficiency of the reduction process, the catalytic activity of the Ag NPs/Zeolite 13X nanocomposite in the reduction of 4-NP was compared separately with untreated zeolite 13X and Ag NPs. No reduction reaction was observed with zeolite 13X after 100 min, which indicates the main role of Ag NPs in the reduction process. In addition, the importance of the support was clearly identified by the longer reaction time achieved with bare Ag NPs which was attributed to the agglomeration of the Ag NPs during the reaction (Table 1). It seems that when Ag NPs/ Zeolite 13X is used, the BH_4^- ion and 4-NP are both absorbed on the catalyst surface. This can facilitate electron transfer from BH_4^- to 4-NP, leading to 4-AP production. In other words, faster electron transfer can occur on the surface of the catalyst, which causes a faster reaction. When Ag NPs/Zeolite 13X nanocomposite was used as a catalyst the λ_{max} at 400 nm gradually decreased and disappeared; the solution became clear in the presence of the catalyst and a new peak appeared at about 295 nm for 4-aminophenol (4-AP). This indicates that 4-NP had converted to 4-AP with increased reaction time [1, 16, 42] (Fig. 10). According to Table 1, the catalytic efficacy increased with an increase in the amount of $NaBH_4$ and

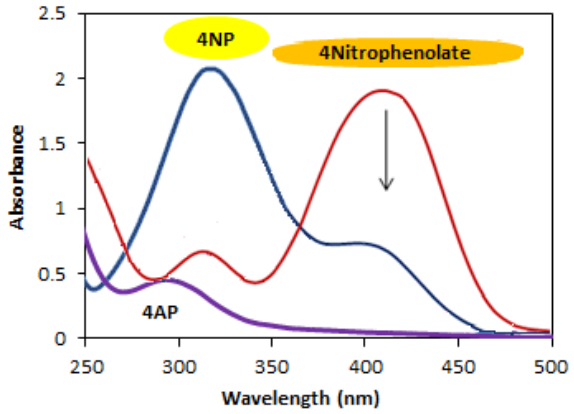

Fig. 10. The UV-Vis spectra of 4-NP aqueous solution in the presence of $NaBH_4$ and Ag NPs/Zeolite 13X nanocomposite

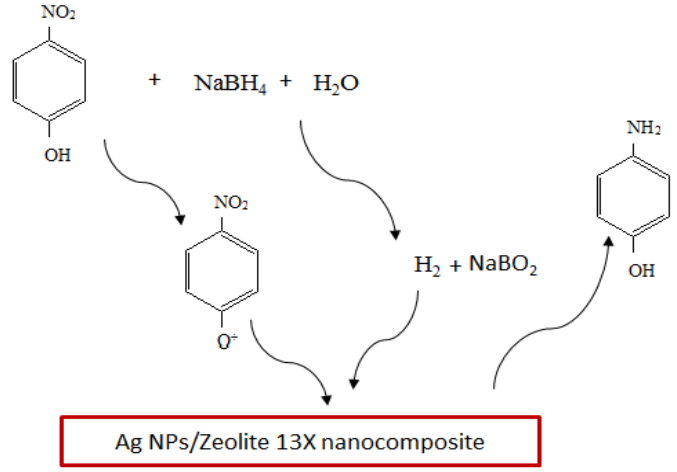

Scheme 4. The proposed mechanism for the reduction of 4-NP to 4-AP in the presence of Ag NPs/Zeolite 13X nanocomposite and $NaBH_4$

catalyst. This means lower reduction times were observed for higher $NaBH_4$ and Ag NPs/ Zeolite 13Xamounts. The best result was obtained using 250 mM (100 equivalents) of $NaBH_4$ and 10.0 mg of catalyst. The reduction process was monitored by using UV-Vis measurements at room temperature, and the results are shown in Fig. 10.

According to the literature, as shown in Scheme 4, the mechanism of the reduction of 4-NP consists of two steps: (1) adsorption of $NaBH_4$ and 4-NP onto the surface of the Ag NPs/Zeolite 13X nanocomposite and (2) electron transfer from BH_4^- to 4-NP through catalyst-mediated reactions and then desorption of 4-AP from the catalyst surface.

The catalytic performance of the Ag NPs/ Zeolite 13X nanocomposite is compared with other reported catalysts and the comparative results are given in Table 2. According to these results, it can be concluded that Zeolite 13X as a support could be employed successfully to decrease Ag NPs agglomeration and to increase the catalyst surface area.

Evaluation of catalytic activity of the Ag NPs/ Zeolite 13X nanocomposite through the reduction of Cr (VI)

The Ag NPs/Zeolite 13X nanocomposite was also used to reduce Cr (VI) in the presence of formic acid. The progress of the reduction reaction was monitored using an indirect UV–visible spectrophotometric method based on the reaction of the remained Cr (VI) and diphenylcarbazid, which forms a red–violet colored complex. Finally, the absorbance of the colored complex was measured in a double-beam spectrophotometer at 540 nm wavelength (Fig. 11) [40].

It is well known that formic acid with potent

Table 2. Comparison of the catalytic performance of the other catalysts in reduction of 4-NP.

Catalyst	Time	Reference
GA-Pt NPs	8 h	[45]
Resin-Au NPs	20 min	[46]
NAP-Mg-Au(0)	7 min	[47]
Ni-PVAm/SBA-15	85 min	[48]
TiO_2-G1%	60 min	[49]
Ag NPs/seashell	4.5 min	[41]
Ag/TiO_2 nanocomposite	2 min	[4]
Ag NPs/Peach kernel shell	1:45 min	[16]
Ag NPs/Zeolite 13X nanocomposite	1:37 min	This work

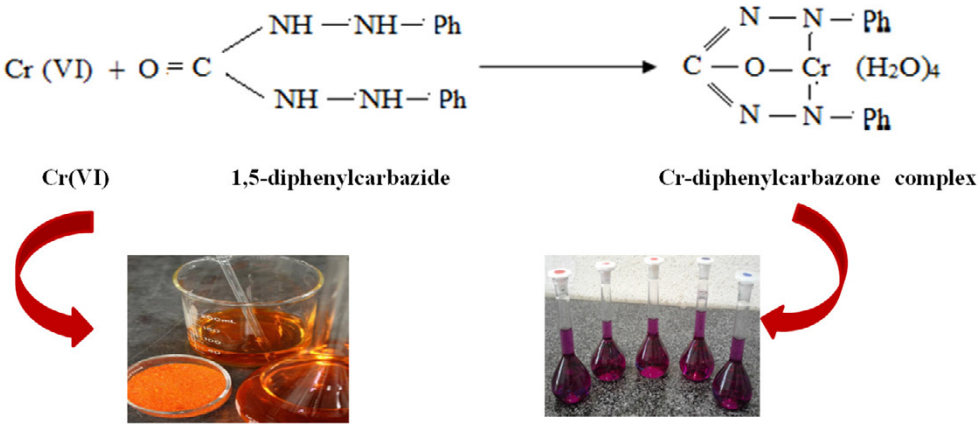

Fig. 11. Structure of 1, 5- diphenylcarbazide and Cr - diphenylcarbaone complex

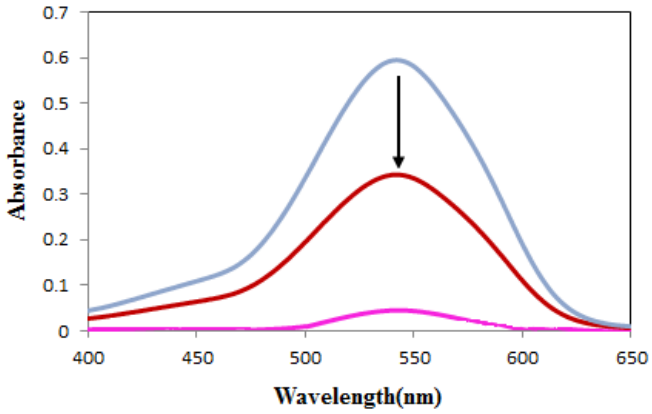

Fig. 12. The UV-Vis spectra of Cr - diphenyl carbaone complex

reducing features in the presence of the nanocatalyst can be easily decomposed to CO_2 and H_2 without the production of intermediate materials [1, 41]. Reduction of Cr (VI) to Cr (III) is accomplished through hydrogen transfer (Scheme 5). As can be seen in Fig. 12, during 10 min, the progress in the reduction of Cr (VI) to Cr (III) is about 97 percent. Optimum conditions included 10.0 mg Ag NPs/Zeolite 13X nanocomposite and 2.0 mL of formic acid.

Catalyst reusability

Obviously, the level of recyclability is an important factor affecting the practical applications

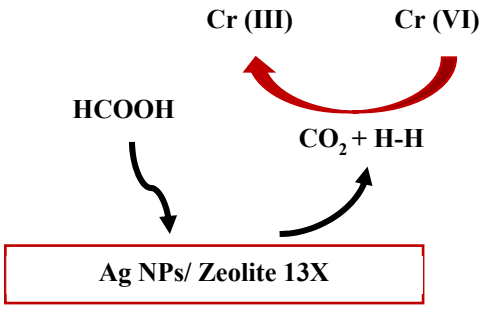

Scheme 5. The proposed mechanism for the reduction of Cr (VI) to Cr (III) in the presence of Ag NPs/Zeolite 13X nanocomposite and Formic acid

of heterogeneous catalysts, especially for commercial and industrial applications. In order to evaluate the reusability of the Ag NPs/ Zeolite 13X, at the end of the reaction, the catalyst was separated from the reaction mixture by brief centrifugation and multiple washings with distilled water followed by drying and reusing in the next cycle. The obtained results showed that the catalyst was reused at least in 6 consecutive cycles for the reduction of 4-nitrophenol without significant loss of catalytic activity, as monitored by UV-Vis spectroscopy. Little decrease of efficiency was observed after the 7th cycle. These results demonstrate the high stability and catalytic activity of the catalyst under the operating conditions. In addition, the catalytic efficiency of the catalyst remained almost constant up to five cycles of operation and the time required for 100% reduction of Cr (VI) was found to be approximately the same up to the 6th cycle.

CONCLUSIONS

In this article, a rapid, convenient, biocompatible and efficient method is developed for the preparation of the Ag NPs and Ag NPs/ Zeolite 13X nanocomposite by Tragopogon graminifolius extract as reducing agent without any stabilizer or surfactant. Moreover, using Tragopogon graminifolius extract, as a bioreducing agent provides a clean, cheap, non-toxic and environmentally benign precursor for the synthesis of the nanocatalyst without using toxic and hazardous reagents and produces non-toxic and less dangerous by-products. SEM, TEM, XRD, EDS, FT-IR and UV-Vis spectroscopic techniques were employed to characterize the synthetic Ag NPs/ Zeolite 13X. Additionally, the green synthesized nanocatalyst exhibited excellent catalytic performance for the reduction of 4-NP and Cr (VI) in water under environmental conditions. The biosynthesized catalyst was stable and easily recycled and reused at least 6 times for 4NP and 5 times for Cr (VI) without sensible loss in its catalytic efficiency.

ACKNOWLEDGMENTS

We gratefully acknowledge the Iranian Nano Council and the University of Qom for the support of this work.

REFERENCES

[1] Nasrollahzadeh M, Sajjadi M, Maham M, Sajadi SM, Barzinjy AA. Biosynthesis of the palladium/sodium borosilicate nanocomposite using Euphorbia milii extract and evaluation of its catalytic activity in the reduction of chromium(VI), nitro compounds and organic dyes. Materials Research Bulletin. 2018;102:24-35.

[2] Zhang W, Xiao X, An T, Song Z, Fu J, Sheng G, et al. Kinetics, degradation pathway and reaction mechanism of advanced oxidation of 4-nitrophenol in water by a UV/H_2O_2 process. Journal of Chemical Technology & Biotechnology. 2003;78(7):788-94.

[3] Nakagawa M, Crosby DG. Photodecomposition of nitrofen. Journal of Agricultural and Food Chemistry. 1974;22(5):849-53.

[4] Atarod M, Nasrollahzadeh M, Sajadi SM. Euphorbia heterophylla leaf extract mediated green synthesis of Ag/TiO_2 nanocomposite and investigation of its excellent catalytic activity for reduction of variety of dyes in water. J Colloid Interface Sci. 2016;462:272-9.

[5] Han Z, Ren L, Cui Z, Chen C, Pan H, Chen J. Ag/ZnO flower heterostructures as a visible-light driven photocatalyst via surface plasmon resonance. Applied Catalysis B: Environmental. 2012;126:298-305.

[6] Khodadadi B, Bordbar M, Yeganeh-Faal A. Optical, structural, and photocatalytic properties of Cd-doped ZnO powders prepared via sol–gel method. Journal of Sol-Gel Science and Technology. 2016;77(3):521-7.

[7] Nasrollahzadeh M, Sajadi SM, Rostami-Vartooni A, Bagherzadeh M, Safari R. Immobilization of copper

nanoparticles on perlite: Green synthesis, characterization and catalytic activity on aqueous reduction of 4-nitrophenol. J Mol Catal A: Chem. 2015;400:22-30.
[8] Nasrollahzadeh M, Sajadi SM, Khalaj M. Green synthesis of copper nanoparticles using aqueous extract of the leaves of Euphorbia esula L and their catalytic activity for ligand-free Ullmann-coupling reaction and reduction of 4-nitrophenol. RSC Adv. 2014;4(88):47313-8.
[9] Pozun ZD, Rodenbusch SE, Keller E, Tran K, Tang W, Stevenson KJ, et al. A systematic investigation of p-nitrophenol reduction by bimetallic dendrimer encapsulated nanoparticles. J Phys Chem C. 2013;117(15):7598-604.
[10] Sivaraj R, Rahman PK, Rajiv P, Narendhran S, Venckatesh R. Biosynthesis and characterization of Acalypha indica mediated copper oxide nanoparticles and evaluation of its antimicrobial and anticancer activity. Spectrochim Acta, Pt A: Mol Biomol Spectrosc. 2014;129:255-8.
[11] Nasrollahzadeh M, Sajadi SM, Rostami-Vartooni A, Bagherzadeh M. Green synthesis of Pd/CuO nanoparticles by Theobroma cacao L. seeds extract and their catalytic performance for the reduction of 4-nitrophenol and phosphine-free Heck coupling reaction under aerobic conditions. J Colloid Interface Sci. 2015;448:106-13.
[12] Bankar A, Joshi B, Kumar AR, Zinjarde S. Banana peel extract mediated novel route for the synthesis of silver nanoparticles. Colloids and Surfaces A: Physicochemical and Engineering Aspects. 2010;368(1):58-63.
[13] Nair LS, Laurencin CT. Silver nanoparticles: synthesis and therapeutic applications. Journal of biomedical nanotechnology. 2007;3(4):301-16.
[14] Lee K-S, El-Sayed MA. Gold and silver nanoparticles in sensing and imaging: sensitivity of plasmon response to size, shape, and metal composition. J Phys Chem B. 2006;110(39):19220-5.
[15] Khodadadi B, Bordbar M, Nasrollahzadeh M. Green synthesis of Pd nanoparticles at Apricot kernel shell substrate using Salvia hydrangea extract: Catalytic activity for reduction of organic dyes. Journal of Colloid and Interface Science. 2017;490:1-10.
[16] Khodadadi B, Bordbar M, Nasrollahzadeh M. Achillea millefolium L. extract mediated green synthesis of waste peach kernel shell supported silver nanoparticles: Application of the nanoparticles for catalytic reduction of a variety of dyes in water. Journal of Colloid and Interface Science. 2017;493:85-93.
[17] Nasrollahzadeh M, Mohammad Sajadi S, Rostami-Vartooni A, Khalaj M. Green synthesis of Pd/Fe_3O_4 nanoparticles using Euphorbia condylocarpa M. bieb root extract and their catalytic applications as magnetically recoverable and stable recyclable catalysts for the phosphine-free Sonogashira and Suzuki coupling reactions. Journal of Molecular Catalysis A: Chemical. 2015;396:31-9.
[18] Petla RK, Vivekanandhan S, Misra M, Mohanty AK, Satyanarayana N. Soybean (Glycine max) leaf extract based green synthesis of palladium nanoparticles. j biomater nanobiotechnol. 2011;3:14-9.
[19] Kurtan U, Baykal A, Sözeri H. Recyclable Fe_3O_4@ Tween20@ Ag nanocatalyst for catalytic degradation of azo dyes. J Inorg Organomet Polym Mater. 2015;25(4):921-9.
[20] Nasrollahzadeh M, Sajadi SM, Rostami-Vartooni A, Khalaj M. Green synthesis of Pd/Fe_3O_4 nanoparticles using Euphorbia condylocarpa M. bieb root extract and their catalytic applications as magnetically recoverable and stable recyclable catalysts for the phosphine-free Sonogashira and Suzuki coupling reactions. J Mol Catal A: Chem. 2015;396:31-9.
[21] Zargar M, Hamid AA, Bakar FA, Shamsudin MN, Shameli K, Jahanshiri F, et al. Green synthesis and antibacterial effect of silver nanoparticles using Vitex negundo L. Molecules. 2011;16(8):6667-76.
[22] Nasrollahzadeh M, Sajadi SM. Synthesis and characterization of titanium dioxide nanoparticles using Euphorbia heteradena Jaub root extract and evaluation of their stability. Ceram Int. 2015;41(10):14435-9.
[23] Chen X, Mao SS. Titanium dioxide nanomaterials: synthesis, properties, modifications, and applications. Chem Rev. 2007;107(7):2891-959.
[24] Laurent S, Forge D, Port M, Roch A, Robic C, Vander Elst L, et al. Magnetic Iron Oxide Nanoparticles: Synthesis, Stabilization, Vectorization, Physicochemical Characterizations, and Biological Applications. Chemical Reviews. 2008;108(6):2064-110.
[25] Suleiman M, Mousa M, Hussein A, Hammouti B, Hadda TB, Warad I. Copper(II)-oxide nanostructures: synthesis, characterizations and their applications-review. Journal of Materials and Environmental Science. 2013;4(5):792-7.
[26] Abdel-Halim E, El-Rafie M, Al-Deyab SS. Polyacrylamide/guar gum graft copolymer for preparation of silver nanoparticles. Carbohydr Polym. 2011;85(3):692-7.
[27] Jassbi AR. Chemistry and biological activity of secondary metabolites in Euphorbia from Iran. Phytochemistry. 2006;67(18):1977-84.
[28] Khodadadi B. Facile sol–gel synthesis of Nd, Ce-codoped TiO2 nanoparticle using starch as a green modifier: structural, optical and photocatalytic behaviors. Journal of Sol-Gel Science and Technology. 2016;80(3):793-801.
[29] Khodadadi B. Effects of Ag, Nd codoping on structural, optical and photocatalytic properties of TiO_2 nanocomposite synthesized via sol-gel method using starch as a green additive. Iran J Catal. 2016;6(3-Special issue: Nanocatalysis):305-11.
[30] Taghavi Fardood S, Ramazani A. Green synthesis and characterization of copper oxide nanoparticles using coffee powder extract. J Nanostruct. 2016;6(2):167-71.
[31] Taghavi Fardood S, Ramazani A, Golfar Z, Joo SW. Green synthesis of Ni-Cu-Zn ferrite nanoparticles using tragacanth gum and their use as an efficient catalyst for the synthesis of polyhydroquinoline derivatives. Appl Organomet Chem. 2017;31(12):e3823.
[32] Taghavi FS, Ramazani A, Golfar Z, Joo S. Green synthesis using tragacanth gum and characterization of Ni-Cu-Zn ferrite nanoparticles as a magnetically separable catalyst for the synthesis of hexabenzylhexaazaisowurtzitane under ultrasonic irradiation. J Struct Chem. 2018;59(7):1789-95.
[33] Fardood ST, Atrak K, Ramazani A. Green synthesis using tragacanth gum and characterization of Ni–Cu–Zn ferrite nanoparticles as a magnetically separable photocatalyst for organic dyes degradation from aqueous solution under visible light. Journal of Materials Science: Materials in Electronics. 2017;28(14):10739-46.
[34] Zarei M, Seyedi N, Maghsoudi S, Nejad MS, Sheibani H. Green synthesis of Ag nanoparticles on the modified graphene oxide using Capparis spinosa fruit extract for catalytic reduction of organic dyes. Inorganic Chemistry Communications. 2021;123:108327.

[35] Khodadadi B, Bordbar M, Yeganeh-Faal A, Nasrollahzadeh M. Green synthesis of Ag nanoparticles/clinoptilolite using Vaccinium macrocarpon fruit extract and its excellent catalytic activity for reduction of organic dyes. Journal of Alloys and Compounds. 2017;719:82-8.
[36] Bordbar M, Sharifi-Zarchi Z, Khodadadi B. Green synthesis of copper oxide nanoparticles/clinoptilolite using Rheum palmatum L. root extract: high catalytic activity for reduction of 4-nitro phenol, rhodamine B, and methylene blue. Journal of Sol-Gel Science and Technology. 2017;81(3):724-33.
[37] Azizi H, Sheidai M, Mozaffarian V, Noormohammadi Z. Genetic and morphological diversity in Tragopogon graminifolius DC.(Asteraceae) in Iran. Cytol Genet. 2018;52(1):75-9.
[38] H Farzaei M, Rahimi R, Abdollahi M. The role of dietary polyphenols in the management of inflammatory bowel disease. Current Pharmaceutical Biotechnology. 2015;16(3):196-210.
[39] Sadeghi A, Bahramsoltani R, Rahimi R, Farzaei MH, Farzaei F, Haghighi ZMS, et al. Biochemical and Histopathological Evidence on Beneficial Effects of Standardized Extract from Tragopogon graminifolius as a Dietary Supplement in Fatty Liver: Role of Oxidative Stress. Journal of Dietary Supplements. 2018;15(2):197-206.
[40] Acar F, Malkoc E. The removal of chromium(VI) from aqueous solutions by Fagus orientalis L. Bioresour Technol. 2004;94(1):13-5.
[41] Rostami-Vartooni A, Nasrollahzadeh M, Alizadeh M. Green synthesis of seashell supported silver nanoparticles using Bunium persicum seeds extract: Application of the particles for catalytic reduction of organic dyes. Journal of Colloid and Interface Science. 2016;470:268-75.
[42] Atarod M, Nasrollahzadeh M, Sajadi SM. Green synthesis of Pd/RGO/Fe_3O_4 nanocomposite using Withania coagulans leaf extract and its application as magnetically separable and reusable catalyst for the reduction of 4-nitrophenol. J Colloid Interface Sci. 2016;465:249-58.
[43] Manonmani V, Juliet V, editors. Biosynthesis of Ag nanoparticles for the detection of pathogenic bacteria in food. Int Conf Innov Manag Serv IPEDR; 2011.
[44] Chen C, Park D-W, Ahn W-S. CO2 capture using zeolite 13X prepared from bentonite. Applied Surface Science. 2014;292:63-7.
[45] Sreedhar B, Devi DK, Yada D. Selective hydrogenation of nitroarenes using gum acacia supported Pt colloid an effective reusable catalyst in aqueous medium. Catal Commun. 2011;12(11):1009-14.
[46] Shah D, Kaur H. Resin-trapped gold nanoparticles: An efficient catalyst for reduction of nitro compounds and Suzuki-Miyaura coupling. Journal of Molecular Catalysis A: Chemical. 2014;381:70-6.
[47] Layek K, Kantam ML, Shirai M, Nishio-Hamane D, Sasaki T, Maheswaran H. Gold nanoparticles stabilized on nanocrystalline magnesium oxide as an active catalyst for reduction of nitroarenes in aqueous medium at room temperature. Green Chem. 2012;14(11):3164-74.
[48] Kalbasi RJ, Nourbakhsh AA, Babaknezhad F. Synthesis and characterization of Ni nanoparticles-polyvinylamine/SBA-15 catalyst for simple reduction of aromatic nitro compounds. Catalysis Communications. 2011;12(11):955-60.
[49] Xu C, Yuan Y, Yuan R, Fu X. Enhanced photocatalytic performances of TiO_2-graphene hybrids on nitro-aromatics reduction to amino-aromatics. RSC Advances. 2013;3(39):18002-8.